JOURNAL OF CATALYSIS 43, 43–52 (1976)

Vapor Phase Oxidation of Ethanol over Thorium Molybdate Catalyst

V. SRIHARI AND D. S. VISWANATH

Department of Chemical Engineering, Indian Institute of Science, Bangalore-560012, India

Received October 12, 1973; revised December 9, 1975

Ethanol oxidation in the vapor phase was studied in an isothermal flow reactor using thorium molybdate catalyst in the temperature range 220–280°C. Under these conditions the catalyst was highly selective to acetaldehyde formation. The rate data were well represented by a steady state two-stage redox model given by the equation:

$$-r = \frac{k_1 k_2 p_E p_{O_2}^{0.5}}{k_2 p_{O_2}^{0.5} + N k_1 p_E}.$$

The parameters of the above model were estimated by linear and nonlinear least squares methods. In the case of nonlinear estimation the sum of the squares of residuals decreased. The activation energies and preexponential factors for the reduction and oxidation steps of the model, estimated by nonlinear least squares technique are: 9.47 kcal/mole, 9.31 g mole/(sec) (g cat) (atm) and 9.85 kcal/mole, 0.17 g mole/(sec) (g cat) $(atm)^{0.5}$, respectively. Oxidations of ethanol and methanol over thorium molybdate catalyst were compared under similar conditions.

INTRODUCTION

Acetaldehyde, the main product of ethanol oxidation, finds use as an intermediate in the manufacture of acetic acid, acetic anhydride, *n*-butanol, pentaerythritol, etc. Commercially it is manufactured either by catalytic vapor phase oxidation or dehydrogenation of ethanol. Silver and copper based catalysts are generally used for oxidation and dehydrogenation routes, respectively. Ethanol oxidation has been studied by several workers with a view to comparing the performance of various catalysts for their activity and specificity. Although there are several studies reported in the literature on this reaction the kinetic data are sparse. Recently, Choudhuri *et al.* (*1*) reported the kinetic data over silver catalyst in the temperature range of 470–570°C and in the high concentration region (23–45% in air) of alcohol. Silver is an expensive material and the temperature involved using silver as catalyst is quite high. It is reported (*2–4*) that in the case of methanol oxidation mixed oxide catalysts, viz, ferric molybdate, vanadium molybdate, manganese molybdate, thorium molybdate, etc., are highly selective to formaldehyde formation and have good activity at relatively lower temperatures (250–350°C). In the present work, in view of the good performance of mixed oxide catalysts for methanol oxidation, thorium molybdate catalyst was explored for ethanol oxidation.

NOMENCLATURE

A	Preexponential factor.
E	Activation energy.
k	Reaction velocity constant.
K	Adsorption equilibrium constant.
m	Order of reaction with respect to ethanol.

N Moles of oxygen required to oxidize 1 mole of ethanol.
n Order of reaction with respect to oxygen.
p Partial pressure, atm.
p_{L_m} Logarithmic mean partial pressure $= (p_i - p_f)/\ln p_i/p_f$, atm.
p_{a_m} Half order mean partial pressure $= (p_i^{0.5} + p_f^{0.5})/2$, atm.
p_i Initial partial pressure, atm.
p_f Final partial pressure, atm.
R' Gas law constant, cal/(mole)(°K).
r Rate of reaction, mole/(sec)(g cat).
T Temperature, °K.
λ Nonintrinsic parameter defined by Eq. (4).

Subscripts

E Ethanol.
G, L Order fixing subscripts
O Oxygen
i *i*th species.

EXPERIMENTAL METHODS

Apparatus, Materials and Methods

An all glass apparatus consisting, mainly, of alcohol vaporizer, air preheater, alcohol–air mixture preheater, reactor and product collection unit (a series of bubblers containing chilled water) was used. A schematic diagram of the apparatus used is shown in Fig. 1. The temperatures at various points in the setup were controlled by autotransformers.

Distilled ethyl alcohol, usually containing 7 mole% water, and air from a constant pressure source were used as starting materials. The air was purified and dried by passing it through a series of towers containing potassium hydroxide, fused calcium chloride, anhydrous calcium sulfate and glass wool. Nitrogen from a high pressure cylinder and of purity over 99% was used, when necessary, after drying.

Thorium molybdate catalyst used in the present investigation was prepared from Analar grade reagents of thorium nitrate [$Th(NO_3)_4 \cdot H_2O$] and ammonium paramolybdate ($NH_4Mo_7O_{24} \cdot 4H_2O$). The bulk density of the catalyst thus prepared was 0.63 g/ml and the average catalyst particle diameter was 0.25 mm with a specific area of 17.6 m^2/g and a pore volume of 0.439 ml/g.

Acetaldehyde was estimated by the excess iodine method recommended by Parkinson and Wagner (*5*). Acetic acid was estimated by titration with standard alkali. Gaseous products were analyzed by the

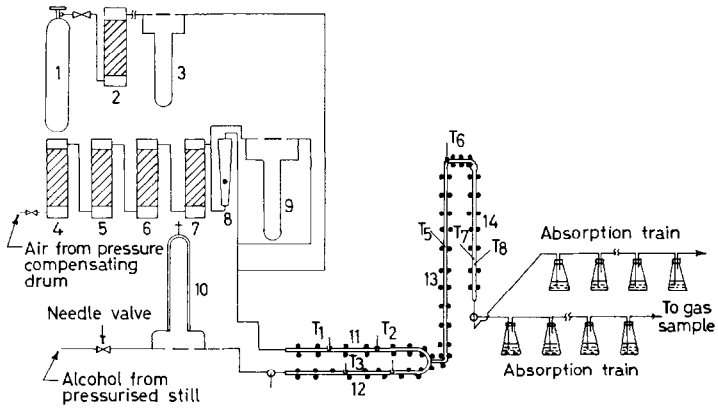

FIG. 1. Schematic diagram of the experimental setup: (1) Nitrogen cylinder; (2 and 5) purifying towers (fused $CaCl_2$); (3) capillary flowmeter for nitrogen; (4) purifying towers (KOH pellets); (6) purifying towers (Dryal); (7) glass wool filter; (8) rotameter for air; (9) capillary flowmeter for air; (10) capillary flowmeter for alcohol; (11) preheater for air; (12) alcohol vaporizer; (13) preheater for alcohol air mixture; (14) reactor; (T_{1-8}) thermometers.

absorptiometric method using the conventional Orsat apparatus.

Before carrying out preliminary studies, a thermodynamic analysis of the reaction,

$$C_2H_5OH + \tfrac{1}{2}O_2 \rightarrow CH_3CHO + H_2O, \quad (1)$$

revealed the irreversible nature of the reaction as at 300°C the equilibrium constant is 1.6×10^{18}. Higher pressures as expected and as reported (*6*) do not favor the reaction.

As the reaction is exothermic the experiments were planned in the low concentration region of ethanol to facilitate easier temperature control. The catalyst was found to be highly selective to acetaldehyde in the temperature range 220–280°C. In this temperature range the only major product formed was acetaldehyde with acetic acid in negligible amounts. Beyond a temperature of 280°C, acetic acid formation increased and also the formation of carbon dioxide was observed. The lower flammable limit of ethanol in air is 4.3 vol%. The maximum concentration of ethanol used in the present work was 2.6 vol%.

Diffusion Effects

Experiments were conducted to find the regions in which resistance due to physical transport phenomena (interphase and intraphase mass diffusion) do not influence the reaction rate. It was found that above a feed flow rate of 240 liters/hr the effect of interphase diffusion on reaction rate is insignificant and that below a particle size of 0.5 mm intraphase diffusion does not influence the reaction rate. For kinetic runs feed flow rates of the order of 400 liters/hr and catalyst particle size of 0.25 mm were used. Theoretical calculations were also made to check the diffusional effects. The influence of interphase diffusion was tested by the method of Yoshida *et al.* (*7*), corresponding to the values of the following variables at 280°C:

Modified Reynolds no. (Re)	6.35
Schmidt no. (Sc)	1.21
Rate no. (R)	8.96×10^{-7}

where the resistance due to external diffusion is more likely to affect the rate. The ratio of partial pressure difference of reactant between bulk phase and catalyst surface to the partial pressure in the bulk phase was found to be 0.00093 indicating the absence of an external diffusion effect. The intraparticle diffusional effect was checked by Weisz and Hicks' method (*8*). For the particle size used the effectiveness factor was found to be close to unity showing the insignificant nature of intraparticle diffusion.

RESULTS AND DISCUSSION

Recent literature on vapor phase oxidations, using transition metal oxides as catalysts, lends considerable support to the reduction–oxidation mechanism. According to this mechanism the oxidation proceeds by simultaneous reduction of the catalyst surface by the reactant and reoxidation by oxygen in the bulk phase. The mechanism can be represented as

$$\text{reactant} + K_{ox} \xrightarrow{k_1} \text{products} + K_{red},$$

$$K_{red} + O_2 \xrightarrow{k_2} K_{ox}.$$

K_{ox} and K_{red} in the above equations represent oxygen ions and vacancies, respectively. The rate equation based on the above mechanism adapted to the present system is:

$$-r = \frac{k_1 k_2 p_E{}^m p_{O_2}{}^n}{k_2 p_{O_2}{}^n + N k_1 p_E{}^m}. \quad (2)$$

Such a mechanism was used (*9–12*) for the oxidation of a variety of compounds. Kulandaivelu (*4*) interpreted his results of methanol oxidation over thorium molybdate catalyst in terms of a steady state two-stage redox model. In view of the considerable support and general applicability of this mechanism, experiments in the present work were planned to test the redox model. The experiments were con-

TABLE 1

Effect of Partial Pressure of Ethanol on Rate, at Constant Oxygen Partial Pressure[a]

Temp (°C)	Mean ethanol partial pressure, p_{E_m} (atm)	Ethanol feed rate, $F_E \times 10^4$ (mole/sec)	Conversion (%)	Rate, $r \times 10^5$ [mole/(sec) (g cat)]
220	0.0030	0.151	18.3	0.0553
	0.0061	0.302	15.9	0.0961
	0.0092	0.453	13.3	0.1207
240	0.0028	0.151	29.1	0.0879
	0.0063	0.277	25.2	0.1674
	0.0081	0.422	23.9	0.2018
	0.0117	0.602	20.5	0.2425
	0.0149	0.755	17.0	0.2565
260	0.0026	0.151	39.9	0.1205
	0.0060	0.277	34.3	0.2279
	0.0083	0.453	30.5	0.2761
	0.0107	0.573	27.4	0.3143
	0.0143	0.755	24.7	0.3726
280	0.0025	0.151	48.0	0.1447
	0.0052	0.302	42.2	0.2550
	0.0078	0.452	40.0	0.3620
	0.0106	0.604	37.5	0.4520
	0.0131	0.724	31.9	0.4630

[a] Catalyst: thorium molybdate; oxygen partial pressure: 0.19 atm; catalyst wt: 5 g; air flow rate: 400 liters/hr.

ducted in a steady state isothermal flow reactor. The effect of variables, ethanol partial pressure, oxygen partial pressure and bed temperature were studied. The following are the ranges of variables covered:

Partial pressure of ethanol 0.0033–0.016 atm

Partial pressure of oxygen 0.018–0.055 atm

Bed temperature 220–280°C

In the ranges of the variables covered, the reaction rate was found to increase with ethanol partial pressure, oxygen partial pressure and bed temperature. Tables 1 and 2 show typical data along with calculated rates. Plots of mean reaction rate against mean partial pressures of ethanol and oxygen with temperature as parameter are shown in Figs. 2 and 3. The two-stage redox equation was integrated for various order combinations and the integrated rate equations can be written as

$$-\frac{1}{r} = \frac{1}{k_1 p_E{}^m(L, G)} + \frac{N}{k_2 p_O{}^n(L, G)}. \quad (3)$$

In Eq. (3), either L or G can be combined with E or O to obtain the four integrated equations. With L the exponent becomes unity and with G it is 0.5.

The data of runs with varying ethanol partial pressure and also that with varying oxygen partial pressure were fitted to integrated redox equations and the constants were estimated by least squares multiple linear regression technique. All the computations were made using an IBM 360/44 computer. Among the four order combinations tried the order combination (1, 0.5) gave the best fit with ±4% deviation. Corresponding to this order combination plots were made of p_{OG}/r vs p_{OG}/p_{EL} for the runs with varying partial pressure of ethanol and of p_{EL}/r vs p_{EL}/p_{OG} for the runs

with varying oxygen partial pressure (Figs. 4 and 5). The plots are linear indicating the validity of the redox model with order combination (1, 0.5). The values of the rate constants estimated for order combination (1, 0.5) are given in Table 3.

Although the redox model gives a good representation of the data, some other models were also tested for their validity for the present system. They are listed in Table 4, and were chosen because of their reported (*13*, *14*) validity in certain oxidation reactions. Initial rate data were used for testing these models. The parameters, were estimated from the linearized equations of the models using the method of least squares. The parameters of the models thus estimated are given in Table 5.

TABLE 2

Effect of Partial Pressure of Oxygen on Rate at Constant Ethanol Partial Pressure[a]

Temp (°C)	Mean partial pressure of oxygen $p_{O_2 m}$ (atm)	Conversion (%)	Rate, $r \times 10^5$ [mole/(sec)(g cat)]
220	0.0180	9.4	0.0569
	0.0271	10.6	0.0638
	0.0361	11.1	0.0672
	0.0452	12.3	0.0741
240	0.0179	16.6	0.0997
	0.0269	18.8	0.1138
	0.0360	20.6	0.1241
	0.0450	21.7	0.1310
	0.0541	22.8	0.1379
260	0.0178	23.1	0.1396
	0.0266	24.8	0.1499
	0.0359	27.1	0.1637
	0.0449	30.0	0.1811
	0.0540	30.8	0.1862
280	0.0267	31.4	0.1897
	0.0358	32.3	0.1948
	0.0448	34.3	0.2069
	0.0539	35.5	0.2138
	0.0630	37.1	0.2241

[a] Catalyst: thorium molybdate; partial pressure of ethanol: 0.0066 atm; catalyst wt: 5 g; ethanol feed rate: 0.302×10^{-4} mole/sec.

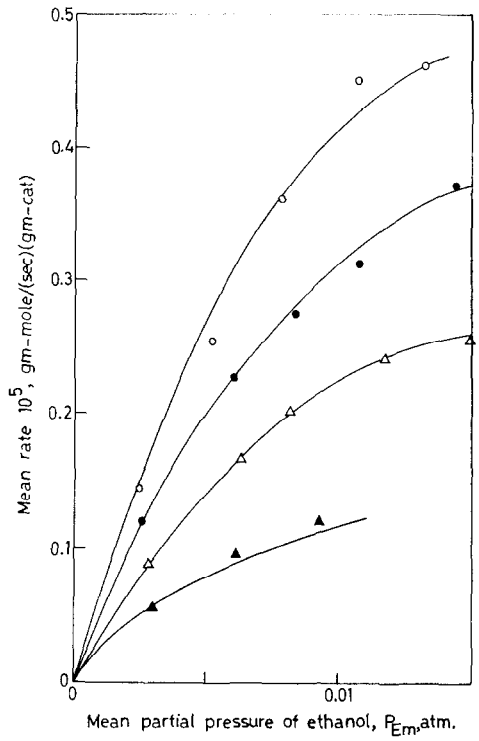

FIG. 2. Rate vs partial pressure of ethanol: (▲) 220°C; (△) 240°C; (●) 260°C; (○) 280°C. Catalyst: thorium molybdate; $p_{O_2} = 0.19$ atm (const.).

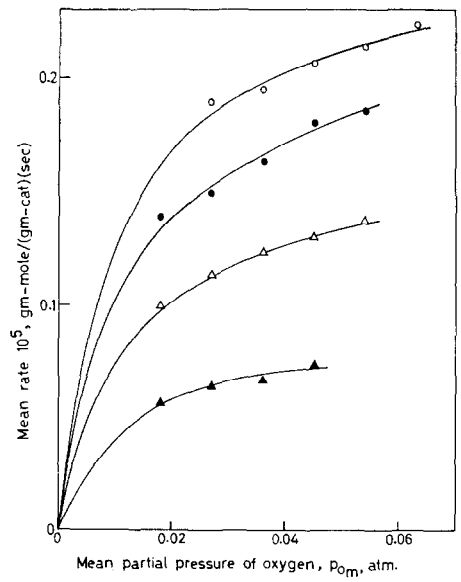

FIG. 3. Rate vs partial pressure of oxygen: (▲) 220°C; (△) 240°C; (●) 260°C; (○) 280°C. Catalyst: thorium molybdate; $p_E = 0.026$ atm.

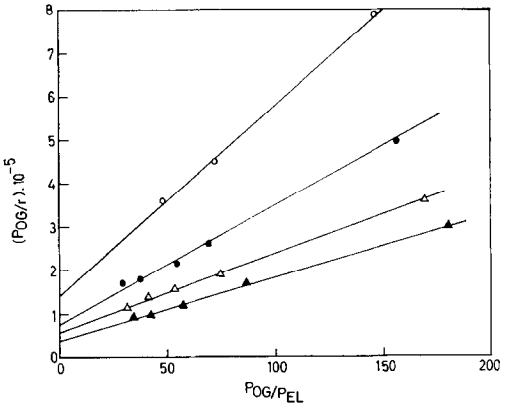

FIG. 4. Plot of p_{OG}/r vs p_{OG}/p_{EL}: (○) 220°C; (●) 240°C; (△) 260°C; (▲) 280°C. Catalyst: thorium molybdate.

For discriminating among different models use is made of the following criteria:

1. Since all constants represent some chemical process they should have positive values to satisfy physical reality.
2. All constants should exhibit temperature sensitivity and be capable of being fitted by an Arrhenius type equation from which activation energies of reaction, adsorption, etc., can be evaluated.
3. A given model should give a good fit to the experimental data.

The summary of the model discrimination can be written as 1(110), 2(111), 3(100), 4(110), 5(100), 6(000), 7(001), 8(000), 9(100), 10(100), 11(110), and 12(110). In this arrangement the number preceding the parentheses represents the model as given in Table 4 and the numbers inside the parentheses show whether the above three criteria are satisfied (indicated by unity), or not satisfied (indicated by zero).

The constants in the different relations as shown in Table 5 were evaluated and the criteria applied. From these it was found that the two-stage redox mechanism gives the best representation. Therefore, all the other models are rejected in favor of the two-stage redox model with order combination of (1, 0.5).

Model discrimination was also made using the statistical method suggested by Mezaki and Kittrel (*15*). This method is based on the estimation of the nonintrinsic parameter λ defined by the equation:

$$Z = \lambda(r_2 - r_1). \tag{4}$$

The quantities r_1 and r_2 represent rates calculated by Models 1 and 2, respectively. Z is a function of experimentally observed rate, r and is given by the equation:

$$Z = r - \tfrac{1}{2}(r_1 + r_2). \tag{5}$$

According to this method for Model 1 to be adequate the confidence interval of λ should include -0.5 and if Model 2 is adequate, the confidence interval of λ should include $+0.5$.

Designating the redox model with order combination (1, 0.5) as Model 1 for discriminating purposes, all the other models were discriminated. The nonintrinsic parameter of each model was estimated using the linear least squares technique and con-

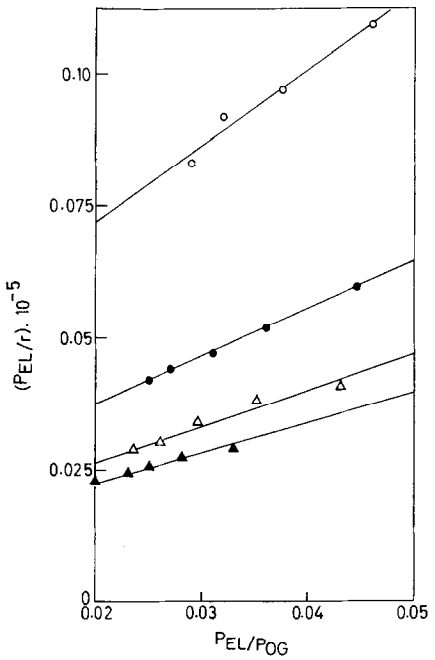

FIG. 5. Plot of p_{EL}/r vs p_{EL}/p_{OG}: (○) 220°C; (●) 240°C; (△) 260°C; (▲) 280°C. Catalyst: thorium molybdate.

TABLE 3

The Magnitudes of Rate Constants, Estimated by Least Squares Linear and Nonlinear Regression, of the Redox Model with Order Combination (1, 0.5)[a]

Temp (°C)	$k_1 \times 10^4$ [mole/(sec)(g cat)(atm)]		$k_2 \times 10^5$ [mole/(sec)(g cat)(atm)$^{0.5}$]		Sum of squares of residuals ($\times 10^{12}$)	
	a	b	a	b	a	b
220	2.25	2.25	0.36	0.35	0.002	0.002
240	3.72	4.11	0.72	0.57	0.118	0.086
260	5.47	5.49	0.94	0.85	0.174	0.088
280	6.97	7.23	1.13	1.12	0.163	0.137

[a] a = linear regression; b = nonlinear regression.

fidence intervals were calculated. Based on the confidence intervals, Models 7, 10, 11 and 12 were rejected and no decision could be taken regarding the other models using this method. However, the other models were rejected based on classical criteria in favor of two-stage redox model with order combination (1, 0.5).

TABLE 4

Models, Other than Two-Stage Redox Model, Tested for Ethanol Oxidation

No.[a]	Model	Model equation	Order combination (m, n)
5	Three-stage redox model	$-r = \dfrac{k_1 p_E^m}{1 + (k_1/k_2)p_E^m + N(k_1 p_E^m/k_3 p_{O_2}^n)}$	(1, 1)
6	Steady state adsorption model with additional assumption that the oxygen desorption rate is not negligible	$-r = \dfrac{k_1 k_2 p_E^m p_{O_2}^n}{k_d + k_2 p_{O_2}^n + N k_1 p_E^m}$	(1, 1)
7	Steady state adsorption model with additional assumption that the oxygen desorption rate is not negligible	$-r = \dfrac{k_1 k_2 p_E^m p_{O_2}^n}{k_d + k_2 p_{O_2}^n + N k_1 p_E^m}$	(1, 0.5)
8	Rideal model	$-r = \dfrac{k K_O p_{O_2}^n p_E^m}{1 + K_O p_{O_2}^n}$	(1, 1)
9	Rideal model	$-r = \dfrac{k K_O p_{O_2}^n p_E^m}{1 + K_O p_{O_2}^n}$	(1, 0.5)
10	Langmuir–Hinshelwood model	$-r = \dfrac{k K_O p_{O_2}^n p_E^m}{(1 + K_O p_{O_2}^n + K_E p_E^m)^2}$	(1, 1)
11	Empirical model	$-r = k p_E^m p_{O_2}^n$	(1, 0.5)
12	Empirical model	$-r = k p_E^m p_{O_2}^n$	(1, 1)

[a] The first four models are those given by Eq. (3).

TABLE 5

Constants of Models Estimated by the Least Squares Method

Model no.	Temp	Magnitude of constants			Av absolute deviation (%)
		$k_1 \times 10^4$	$k_2 \times 10^5$		
1	220	1.83	2.82		6.8
	240	3.09	5.72		8.0
	260	4.49	7.52		9.6
	280	5.93	7.27		7.2
2	220	2.25	0.36		1.3
	240	3.72	0.72		3.7
	260	5.47	0.94		3.5
	280	6.97	1.13		2.5
3	220	0.12	4.14		6.6
	240	0.20	8.33		8.6
	260	0.28	11.31		8.8
	280	0.35	10.85		12.1
4	220	0.13	0.51		8.6
	240	0.22	1.16		12.2
	260	0.31	1.54		12.3
	280	0.38	1.90		15.1
		$k_1 \times 10^6$	$k_2 \times 10^4$	$k_3 \times 10^5$	
5	220	2.95	2.48	3.21	4.4
	240	7.57	3.78	5.72	3.3
	260	9.92	5.57	7.33	4.7
	280	22.99	6.60	6.26	6.1
		$k_1 \times 10^4$	$k_2 \times 10^6$	$k_d \times 10^7$	
6	220	1.60	6.22	−4.20	4.4
	240	2.85	14.73	−6.91	3.3
	260	4.08	19.21	−9.81	4.7
	280	5.56	30.72	−9.23	6.1
7	220	2.22	2.88	−1.26	3.1
	240	3.94	6.76	0.96	1.9
	260	6.00	8.90	2.34	1.6
	280	9.42	14.30	25.84	4.0
		$k \times 10^5$	$K_O \times 10$		
8	220	9.22	−4.21		16.8
	240	16.99	−4.66		17.4
	260	22.96	−4.26		17.7
	280	28.24	−4.05		11.8
9	220	2.87	3.16		14.7
	240	4.54	3.83		13.5
	260	7.05	3.13		14.9
	280	11.43	1.92		12.3
		$k \times 10^6$	$K_O \times 10^2$	$K_E \times 10^2$	
10	220	7.68	0.19	1.82	78.6
	240	18.82	0.14	0.98	84.0
	260	26.99	0.14	0.95	81.7
	280	50.73	0.08	0.53	90.9
		$k \times 10^4$			
11	220	6.66			50.0
	240	11.27			48.6
	260	16.24			46.9
	280	22.45			41.0
12	220	2.98			34.0
	240	5.02			34.4
	260	7.21			31.9
	280	9.82			24.5

Having found the two-stage redox model with order combination (1, 0.5) to represent the data adequately, the parameters of the rate equation corresponding to this model were estimated by the nonlinear least squares estimation technique. The parameters thus estimated are given in Table 3. It is seen from the table that use of the nonlinear least squares technique has resulted in a decrease of sum of squares of residuals.

Temperature Dependence of Rate Constants

The rate constants when plotted showed that they followed the Arrhenius law. The activation energy and preexponential factor were estimated both by the linear and nonlinear least squares techniques. In the nonlinear estimation the reparameterized temperature was used, as suggested by Peterson (*16*). The Arrhenius equation is modified as:

$$k = A' \cdot \exp(-E/R'T'), \qquad (6)$$

where

$$\frac{1}{T'} = \frac{1}{T} - \frac{1}{\bar{T}},$$

and

$$\frac{1}{\bar{T}} = \frac{1}{nt} \sum_{i=1}^{nt} \frac{1}{T_i};$$

nt in the above equation represents the number of temperature levels. The activation energy and preexponential factor estimated by the linear and nonlinear methods are presented in Table 6. It is seen that in this case also the sum of squares of residuals has decreased in the case of the nonlinear estimation method.

Comparison of Ethanol and Methanol Oxidations over Thorium Molybdate Catalyst

Data on methanol oxidation were also collected. The rate data on methanol oxida-

TABLE 6

Activation Energy and Preexponential Factor Estimated by Linear and Nonlinear Regression

A_1 [mole/(sec) (g cat)(atm)]	E_1 (kcal/mole)	Sum of squares of residuals ($\times 10^8$)	A_2 [mole/(sec) (g cat)$(atm)^{0.5}$]	E_2 (kcal/mole)	Sum of squares of residuals ($\times 10^{12}$)
		Linear regression			
9.30	10.34	0.41	0.17	10.05	0.42
		Nonlinear regression			
9.47	9.31	0.27	0.17	9.85	0.29

tion over thorium molybdate catalyst were well represented by the two-stage redox model with $m = 1$ and $n = 0.5$. The rate constant and activation energy data for ethanol and methanol oxidations under the same conditions are presented in Table 7. The activation energies obtained by Kulandaivelu (*4*) in the case of methanol oxidation over thorium molybdate catalyst are also given in Table 7 and our values compare well with them. Ethanol oxidizes more rapidly than methanol since the rate constant k_1 for ethanol oxidation is higher than that for methanol oxidation and the activation energy for ethanol oxidation (9.3 kcal/mole) is less than that for methanol oxidation (15.5 kcal/mole).

In alcohol oxidation the reaction takes place either by the disruption of the RO–H bond or the RC(OH)–H bond. The energy of disruption involved in the disruption of the RO–H bond in different alcohols is reported (*17*) to be the same. But the energy required for disrupting the RC(OH)–H bond in ethanol (about 88 kcal/mole) is reported (*18*) to be smaller than that required for the methanol molecule (about 92 kcal/mole). This may be the reason for the higher reactivity and lower activation energy for ethanol oxidation in comparison with methanol oxidation. A similar observation was made by Evmenenko and Gorokhovatskii (*19*) in comparing the oxidations of ethanol and methanol on ferromolybdenum catalyst.

TABLE 7

Comparison of Rate Constants and Activation Energies of Methanol and Ethanol Oxidations on Thorium Molybdate Catalyst

System	Temp (°C)	$k_1 \times 10^4$ [mole/(sec) (g cat)(atm)]	$k_2 \times 10^5$ [mole/(sec) (g cat)$(atm)^{0.5}$]	E_1 (kcal/mole)	E_2 (kcal/mole)
Methanol oxidation	260	3.01	2.44	15.5	22.3
	280	5.95	4.05	15.7[a]	20.5[a]
Ethanol oxidation	260	5.49	0.85	9.3	9.8
	280	7.23	1.12		

[a] Values reported by Kulandaivelu (*4*).

REFERENCES

1. Choudhuri, A. K., Sengupta, P., and Roy, N. C., presented: 24th Annu. general meeting of Indian Inst. of Chem. Eng., Kanpur, 1972.
2. Mann, R. S., and Hahn, K. W., *J. Catal.* **15**, 329 (1969).
3. Dente, M., Poppi, R., and Pasquon, I., *Chim. Ind.* **46**, 1326 (1964).
4. Kulandaivelu, V., PhD thesis, Indian Institute of Science, Bangalore, 1971.
5. Parkinson, A. E., and Wagner, E. C., *Ind. Eng. Chem. Anal. Ed.*, **6**, 433 (1934).
6. Patterson, J. A., and Day, A. R., *Ind. Eng. Chem.* **26**, 1276 (1934).
7. Yoshida, F., Ramaswamy, Y., and Hougen, O. A., *AIChE J.* **8**, 5 (1962).
8. Weisz, P. B., and Hicks, J. S., *Chem. Eng. Sci.* **17**, 265 (1962).
9. Mars, P., and Van Krevelen, D. W., *Chem. Eng. Sci.* (Special Suppl.) **3**, 41 (1954).
10. Firth, J. G., and Holland, H. B., *Trans. Faraday Soc.* **65**, 189 1 (1969).
11. Šimeček, A., Kadlec, B., and Michálek, J., *J. Catal.* **14**, 287 (1969).
12. Dwyer, F. G., *Catal. Rev.* **6**, 264 (1972).
13. Legendre, M., and Cornet, D., *J. Catal.* **25**, 194 (1972).
14. Saito, H., *J. Chem. Soc. (Japan), Pure Chem. Sect.* **71**, 133–5 (1950).
15. Mezaki, R., and Kittrel, J. R., *Canad. J. Chem. Eng.* **44**, 285 (1966).
16. Peterson, T. I., *Chem. Eng. Sci.* **17**, 203 (1962).
17. Mortimer, C. T., "Reaction Heats and Bond Strengths," p. 136. Pergamon, New York, 1962.
18. Vedeneev, V. I., Gurvich, L. V., Kondratev, V. N., Medvedev, V. A., and Frankevich, E. Y., "Energy of Disruption of Chemical Bonds, Ionization Potentials and Affinity for Electrodes," Iz. Akad. Nauk SSSR, Moscow, 1962.
19. Evemenenko, N. P., and Gorokhovatskii, Y. B., *Kinet. Katal.* **11**, 130 (1970).